JPPIPA 9(10) (2023)

Jurnal Penelitian Pendidikan IPA

Journal of Research in Science Education

http://jppipa.unram.ac.id/index.php/jppipa/index

Analysis of the Effect of Local Magnitude on Peak Ground Acceleration and Seismic Vulnerability Index for Geothermal Field Monitoring Using Microearthquake

Widya Utama[1*], Rista Fitri Indriani[2], Sherly Ardhya Garini[3]

[1] Department of Geophysics Engineering, Institut Teknologi Sepuluh Nopember, Surabaya 60111, Indonesia.
[2] Department of Geomatics Engineering, Institut Teknologi Sepuluh Nopember, Surabaya 60111, Indonesia.
[3] Department of Informatics, Institut Teknologi Sepuluh Nopember, Surabaya 60111, Indonesia.

Received: April 27, 2023
Revised: September 15, 2023
Accepted: October 25, 2023
Published: October 31, 2023

Corresponding Author:
Widya Utama
widya@gaofisika.its.ac.id

DOI: 10.29303/jppipa.v9i10.3743

Abstract: Intensive exploitation of geothermal injection and production can trigger microearthquakes which it signals come from dynamic fractures. The purpose of this study is to decide the impact of local magnitude on mitigation in geothermal fields based on soil acceleration and vulnerability of seismic in geothermal fields. This study uses seismic wave recording data and the geology of the research area. It is focable on calculating local magnitude, ground acceleration and seismic susceptibility index to earthquakes based on ground acceleration and seismic susceptibility index in geothermal fields. The maximum amplitude value represent that the medium classification class ($3<A_0<6$) is associated with a moderate degree of deformation. Natural frequency value are found with a moderate classification ($4<f_0<10$) around the area of injection wells and production wells, indicating that the research area has a moderate level of soil hardness structure. The peak ground acceleration in the study area is classified as moderate ($0.25<PGA<0.7$) which means that the area has a moderate level of risk. Vulnerability of seismic in the study area is included in the low classification ($Kg<10$). The local magnitude impact on soil acceleration and vulnerability of seismic in this study has a moderate risk and can be categorised as safe. In the future, this research serves as a basis for proper decision-making in geothermal energy operations, monitoring, and infrastructure development.

Keywords: Geothermal; Local Magnitude; Microearthquakes; Monitoring; Seismic

Introduction

Geothermal reservoir dynamics can be characterized by microearthquake activity. Microearthquake study is a best practice method, widely able by geothermal companies as part of Engineered Geothermal System (EGS). Intensive production and injection exploitation activities affect anisotropy conditions because its transformation fluid pressure in the pores which has the potential to impact new pore spaces (fractures) to open, reservoir volume transformation, and reservoir temperature decreases as part of a continuous reservoir, monitoring and evaluation (Hopp et al., 2019). Precise information from the region of the microearthquake hypocenter contributes to the understanding of geothermal reservoir activity. However, a bias can be found between the hypocentral parameters (quality of wave phase arrival time, number and placement of seismic stations, azimuth placement, etc.) and the subsurface seismic velocity model for the cluster area which contributes to the uncertainty of seismic fracture mapping and region. geothermal reservoir area (Midzi et al., 2020).

In the preliminary study, the hypocenter region was improved using the Double Difference (DD) method and integrated with the coherence factor between hypocenters (Sevilla et al., 2020; Utama et al., 2020). Furthermore, the local magnitude (ML) value is computed for each microearthquake around the geothermal field reservoir area starting from

How to Cite:
Utama, W., Indriani, R. F., & Garini, S. A. (2023). Analysis of the Effect of Local Magnitude on Peak Ground Acceleration and Seismic Vulnerability Index for Geothermal Field Monitoring Using Microearthquake. *Jurnal Penelitian Pendidikan IPA*, *9*(10), 7855–7864. https://doi.org/10.29303/jppipa.v9i10.3743

determining and testing the region of the hypocenter (Bulo et al., 2020). Computation of ground acceleration is carried out from the magnitude and radius of the epicenter. While vulnerability of seismic is based on the maximum amplitude and natural frequency (Dwiyanti et al., 2020). The purpose of this research is to determine the impact of local magnitude on mitigation in geothermal fields based on peak ground acceleration and seismic vulnerability in geothermal fields. The novelty of this research is the integrated application through the calculation of regional local magnitude, peak ground accelaration, and seismic vulnerability index in geothermal areas. This research is important in the improvement, enhancement, utilization of geothermal energy, and seismic hazard management due to intensive exploitation activities in the geothermal field in the future such as hydraulic fracturing that causes fractures around the geothermal exploration area (Nezhad et al., 2021).

Method

This research specifically focable on identification of the local magnitude impact towards seismicity based on the peak ground acceleration and vulnerability of seismic in geothermal fields.

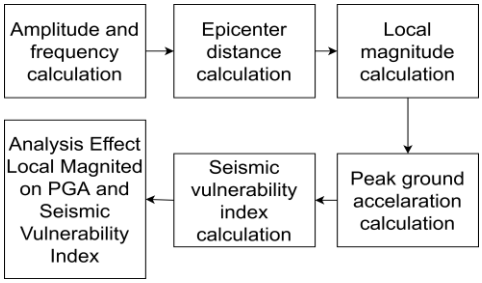

Figure 1. Research Flowchart

This study uses seismic wave recording data and the range time of the earthquake. The data able are 277 earthquake data and 7 seismic wave recording stations. Recorded data with a period of 30 days and researched in the geothermal field of West Java province (Foytong & Ornthammarath, 2020).

Computation of Maximum Amplitude (A_0) and Natural Frequency (f_0)

The Geopsy is able in data processing to decide the maximum amplitude using microearthquake.mxd data. The steps in Geopsy are changing the components in the data, then inputting the wave-picking parameter with windowing for the wave smoothing parameter from the Floor Spectral Ratio noise and picking the data. There is a spectral analysis in Geopsy data processing. FSR (Floor Spectral Ratio) analysis was done using Geopsy software, the first step is by conducting Fourier spectrum analysis which was done to convert the initial microearthquake data from a time domain (time series) to a frequency domain (Jun et al., 2023; Shim et al., 2023). Each recording length of the Fast Fourier Transform (FFT) algorithm in spectrum analysis separated into 0 to 15 seconds of non-overlapping window. Konno and Ohmachi smoothing filters are able to get smoother results from FFT process with a bandwidth coefficient of 40. The average amplitude spectrum for each component is computed from the selected window (Maimun et al., 2020). Then, the maximum amplitude and natural frequency values are accomplished from this stage (Mihaylov et al., 2019).

Epicenter Radius Computation

Isotropic homogeneous is assumed as the medium able in this study. In this medium, the earthquake waves propagate as rays and straight lines. The earthquake waves that propagate on the earth's structure consists of many layers at a constant speed will approach at the earthquake recording station in three ways, namely direct waves, reflected waves and refracted waves. It is complementary to the hypocenter radius, epicenter radius, and constant wave velocity in isotropic homogeneous medium (Sungkowo, 2018).The succeeding is the formula for calculating hypocenter radius:

$$JH = \sqrt{(X_2 - X_1)^2 + (Y_2 - Y_1)^2} \quad (1)$$

With JH as hypocenter radius (km), while X and Y as the coordinate of station and hypocenter point. The succeeding is an illustration of epicenter radius computation in Figure 2.

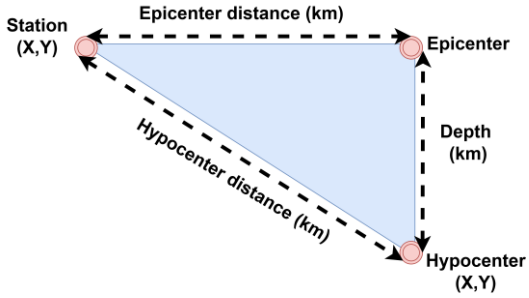

Figure 2. Illustration of epicenter radius computation (Sungkowo, 2018)

From the illustration above, the Pythagorean formula is able to compute the epicenter radius with the succeeding formula:

$$JH = \sqrt{Z^2 + JE^2} \quad (2)$$

$$JE = \sqrt{Z^2 - JH^2} \quad (3)$$

With JH as the epicenter radius (km), Z as the deepness (km), and JE as epicenter radius (km) (Liu et al., 2022; Zhou et al., 2022).

Local Magnitude Computation

The local magnitude (ML) determines the radius from the epicenter to the seismograph and measures the maximum amplitude of the signal recorded on the seismograph, so that an approach can be done to determine the magnitude of the earthquake that occurs. (Lobos Lillo et al., 2023; Okamoto et al., 2022; Tang et al., 2023). The local magnitude has the empirical formula as follows:

$$M = \log a + 2.76 \log D - 2.48 \quad (4)$$

With a as the amplitude of ground vibration, D as the radius between recording station and the epicenter (km) with D <600 km (Bulo et al., 2020).

Peak Ground Acceleration Computation

The peak ground acceleration is the wave acceleration that reaches the earth's surface. The peak ground acceleration in a particular area which computed from the impact of vibration within a certain time and also by considering the magnitude value, epicenter radius, and period value (Xie et al., 2021). The computation of ground acceleration value can be done from several Tong and Katayama equations as follows:

$$\log \overline{PGA} = \alpha M - \beta \log JE + \gamma T + \delta \quad (5)$$

With T as the period of time, M as the magnitude, JE as epicenter radius, and α=0.509, β=2.32, γ=0.039, δ=2.33 (Cao et al., 2023; Hendra et al., 2019; Hofmann et al., 2021).

Computation of Vulnerability of Seismic

Vulnerability of seismic is presented as a number that express vulnerability of the surface soil layer due to transformation in the condition of the soil layer during an earthquake/vibration (Guglielmi et al., 2023).

$$VI = \frac{{A_0}^2}{f_0} \quad (6)$$

With VI as the vulnerability of seismic, A_0 as the maximum amplitude, and f_0 as natural frequency (Núñez et al., 2022; Yoo et al., 2021).

Result and Discussion

The maximum amplitude, natural frequency, epicenter radius, local magnitude, and maximum acceleration have been accomplished in this research. The result of microearthquakes data processing is presented as follows.

Results of Maximum Amplitude (A_0) and Natural Frequency (f_0)

The Geopsy was able to determinate maximum amplitude. There are 277 event data that able in this study. The maximum amplitude is capable by deformation. Natural frequency illustrates the level of soil structure hardness (Ahn et al., 2021; Zhu et al., 2020). The succeeding is the event data able:

Table 1. Computation of Maximum Amplitude and Natural Frequency

Recording	A0	f0
20180101 22	5.18	11.48
	4.32	7.32
	8.30	1.49
	7.18	5.91

Understanding the seismic behavior in geothermal areas holds significant importance for both scientific investigation and practical implementation, particularly with regards to the well-being of infrastructures and communities. In this particular investigation, an extensive examination was carried out on the utmost magnitude and inherent frequency linked to seismic incidents of localized magnitude within a geothermal region. The primary objective of this analysis was to unravel the intricate interplay between geological characteristics, tectonic pressures, and geothermal operations, all of which exert an influence on seismic activity (Esquivel-Mendiola et al., 2022; Li et al., 2023; Zhang et al., 2023).

The examination of maximum magnitudes recorded in the seismic records offers valuable insights into the magnitude of seismic events in the geothermal region. The detection of elevated magnitudes can serve as an indication of substantial energy release during seismic activities. Our discoveries unveiled a correlation between elevated magnitudes and specific geological characteristics such as fault lines and areas with heightened tectonic stress. These observations align with existing literature, suggesting that regions characterized by geological faults have a tendency to display higher seismic magnitudes due to the sudden release of accumulated stress along these fault lines. The maximum amplitude distribution map presented in Figure 3 (Keil et al., 2022; Wamriew et al., 2022).

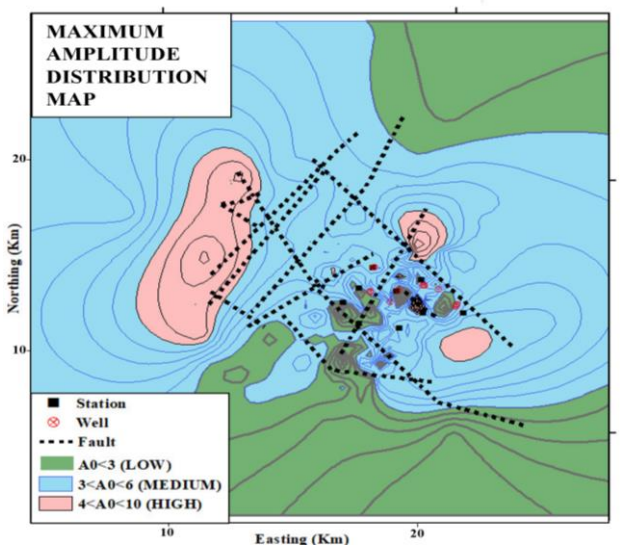

Figure 3. Maximum Amplitude Distribution Map

The examination of natural frequencies linked to seismic occurrences yields significant insights into the fundamental geological configurations. The natural frequencies are impacted by the elastic characteristics of rocks and the distribution of stress within the Earth's crust. Our investigation disclosed clear-cut frequency ranges that align with distinct geological formations within the geothermal region. These discoveries exhibit conformity to the resonance phenomenon, whereby specific geological structures intensify seismic waves at specific frequencies.and the natural frequency distribution map are presented in Figure 3 and Figure 4 (Elbshbeshi et al., 2022).

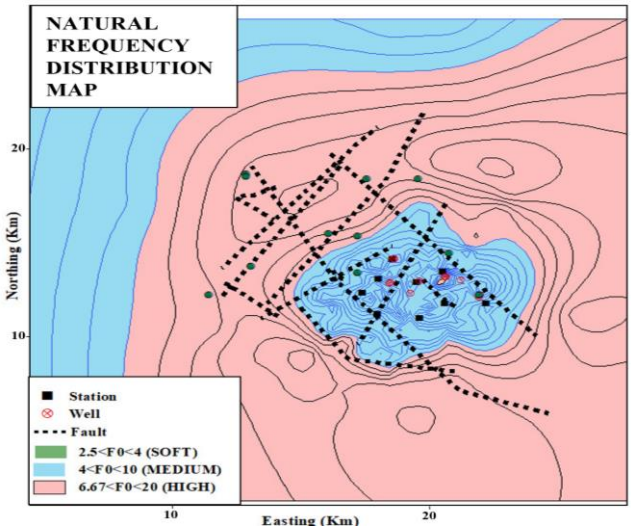

Figure 4. Natural Frequency Distribution Map

Epicenter Radius Results

Epicenter radius computation shows the radius between hypocenter and epicenter. The succeeding is the result from the recordings:

Table 2. Computation of Epicenter Radius

Recording	Hypocenter radius (km)	Z (km)	Epicenter radius (km)
20180101 22	1.68	0.4	1.63
	1.06	0.4	0.98
	2.23	0.4	2.2
	2.27	0.4	2.24

The epicenter radius shows the radius from the earthquake's epicenter to the station. Epicenter analysis also serves as an indicator of ongoing geothermal activity. Seismic events located in close proximity to known geothermal reservoirs or vents suggest a strong connection between geothermal processes and seismicity. The movement of geothermal fluids can induce seismic events, highlighting the dynamic nature of geothermal systems (Andinisari et al., 2021; Ryu et al., 2022; Yue et al., 2023).

Local Magnitude Results

The local magnitude is computed by considering epicenter radius and the maximum amplitude value. The succeeding is the result of the magnitude computation:

Table 3. Computation of Local Magnitude

Recording	Local magnitude	Local magnitude event
20180101 22	1.18	1.08
	1.87	
	0.62	
	0.66	

The recorded data illustrates that the local event magnitude is 1.08. The magnitude is affected by the maximum amplitude and the radius from the epicenter (Bulo et al., 2020). The local magnitude of the event is accomplished from the average value of the local magnitude from each station. The local magnitude distribution map is shown in Figure 5. Investigating the regional scale of seismic occurrences in connection with geothermal energy offers irreplaceable comprehension into the interplay between tectonic pressures and geothermal procedures. Earthquakes are frequently initiated or impacted by the motion of geothermal fluids, rendering the assessment of the regional scale an indispensable instrument for overseeing these operations (Lobos Lillo et al., 2023; Okamoto et al., 2022; Tang et al., 2023).

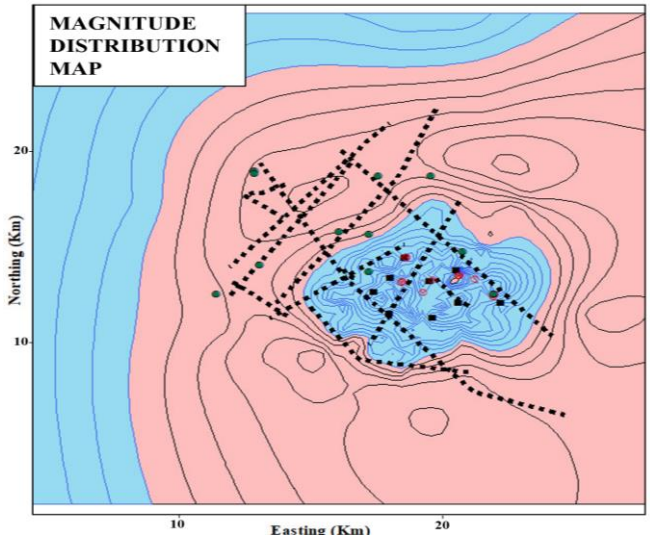

Figure 5. Magnitude Distribution Map

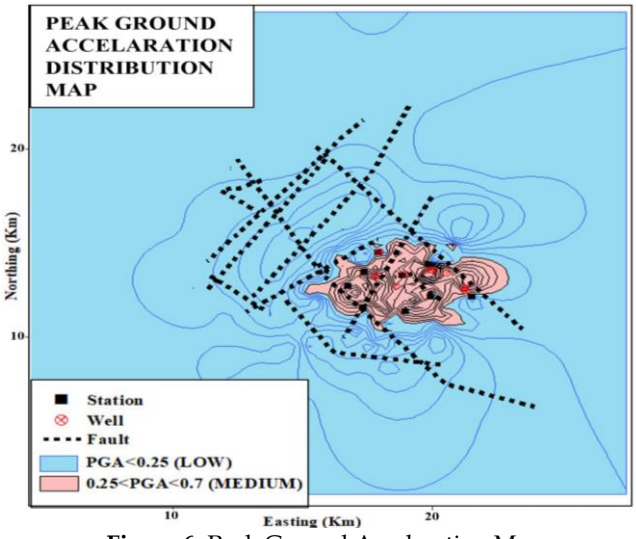

Figure 6. Peak Ground Acceleration Map

Peak Ground Acceleration Results

The peak ground acceleration of an area is computed from the impact of vibration within a certain time and by considering the magnitude value, hypocenter radius, and the period value. The succeeding is the computation result of peak ground acceleration:

Table 4. Computation of Peak Ground Acceleration

Recording	PGA	PGA event
20180101 22	0.46	0.41
	0.87	
	0.15	
	0.15	

In the recorded data, the ground acceleration of the event is 0.41. The event ground acceleration is accomplished from the average ground acceleration value of each station. The distribution map of peak ground acceleration is shown in Figure 6 (Keil et al., 2022).

PGA values represent the maximum ground acceleration encountered during an earthquake and are of utmost importance for the quantification of seismic hazard. In geothermal regions, where seismic activity is frequently influenced by both tectonic forces and geothermal processes, accurate evaluation of PGA is indispensable. High PGA values indicate vigorous ground shaking, which can present significant dangers to infrastructure, particularly in areas where geothermal energy extraction is in progress. Through precise quantification of PGA, scientists are able to classify the degree of seismic hazard, facilitating the implementation of appropriate safety measures and regulations for geothermal operations (Kim et al., 2018; Kowsari et al., 2021; Ramirez et al., 2022; Tao et al., 2021).

Vulnerability Index of Seismic Results

Vulnerability index or vulnerability seismic index is affected by the value of maximum amplitude and natural frequency. The evaluation of the seismic vulnerability index, which serves as a crucial measure in assessing the potential impact of earthquakes on structures and communities, is significantly influenced by a range of seismic parameters. Among these parameters, maximum amplitude and natural frequency emerge as key factors that play substantial roles. This analysis delves into the intricate connection between these parameters and the seismic vulnerability index, shedding light on the implications for earthquake preparedness, structural design, and strategies for mitigating risk (Kim et al., 2018; Kowsari et al., 2021; Tao et al., 2021).

The maximum amplitude, which represents the highest level of ground motion experienced during an earthquake, directly affects the destructive potential of seismic events. Greater amplitudes correspond to more intense shaking, resulting in heightened structural stress and the possibility of damage. Structures situated in regions with high maximum amplitudes are inherently more susceptible to the impact of seismic events. By incorporating maximum amplitude values into the seismic vulnerability index, it becomes possible to identify areas where structures face greater risk. This prompts the implementation of stricter building codes and retrofitting measures (Alkan & Akkaya, 2023; Mahjour & Faroughi, 2023).

The natural frequency, determined by geological and structural properties of an area, represents the inherent vibrational frequency of buildings and infrastructures. When the frequency of seismic waves aligns with the natural frequency of a structure, resonance can occur, amplifying ground motion and consequently leading to structural damage.

Consequently, areas with specific natural frequencies are more prone to the effects of resonance, thereby heightening the vulnerability of buildings and bridges. Understanding the natural frequency of both the ground and structures is vital in the design of earthquake-resistant buildings and the mitigation of vulnerabilities related to resonance (Gori et al., 2023). The result of seismic vulnerability value is as follows:

Table 5. Computation of vulnerability of seismic

Recording	Vulnerability index	Vulnerability index event
20180101 22	2.34 2.55 46.23 8.72	14.96

The recorded data shows seismic event vulnerability index of 14.96. Seismic event susceptibility index is accomplished from the average value of the vulnerability of seismic for each station. Then distribution map of vulnerability of seismic is shown in Figure 7 (Elbshbeshi et al., 2022).

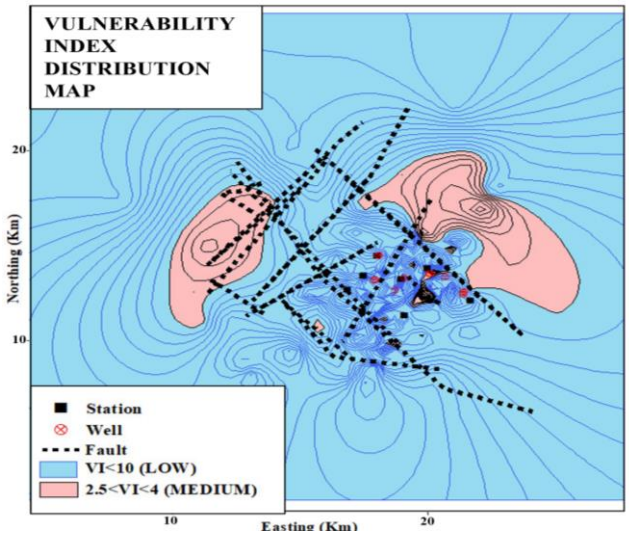

Figure 7. Vulnerability Index Distribution Map

Incorporation of the maximum amplitude and natural frequency data into the seismic vulnerability index results in a more nuanced and accurate evaluation of the potential impact of earthquakes. The inclusion of these parameters renders the vulnerability index a comprehensive tool, which takes into account not only the seismicity of the region but also the specific characteristics of structures and the geological formations on which they are situated. This integrated approach empowers authorities and engineers to allocate resources efficiently by prioritizing areas with heightened vulnerabilities, and implement targeted interventions to enhance the resilience of critical infrastructure and communities (Gori et al., 2023; Mahjour & Faroughi, 2023).

Discussion

The research outcomes offer significant and precious understandings into the seismic features of the geothermal area. Specifically, they shed light on the local magnitude (ML), peak ground acceleration (PGA), and the seismic vulnerability index. This comprehensive discussion delves deeply into the implications of these findings, placing particular emphasis on the intricate and subtle relationship that exists between these parameters. Furthermore, it explores the collective influence of these parameters on various aspects of seismic risk assessment, including infrastructure resilience and geothermal operations. The multifaceted nature of this relationship is thoroughly examined and analyzed, providing valuable insights and knowledge in these areas (Gori et al., 2023; Mahjour & Faroughi, 2023).

The act of classifying seismic events into two distinct categories, namely microearthquakes and ultra-microearthquakes, serves to emphasize the presence of seismic activities in the region that may otherwise go unnoticed due to their subtle nature (Hopp et al., 2020; Kinscher et al., 2023; Nibe & Matsushima, 2021). By specifically identifying microearthquake zones in close proximity to injection and production wells, it becomes apparent that seismicity is localized to these areas. The fact that these zones exhibit moderate maximum amplitude values, which are indicative of their deformation capability, suggests that there is a moderate level of ground deformation potential during seismic events within these specific areas. This potential for deformation, when combined with the presence of specific geological features such as pyroclastic andesite lava lithology, highlights the necessity for careful and thorough evaluation in both the design of structures and the planning of geothermal infrastructure. The intricate nature of these factors necessitates a meticulous approach in order to ensure the safety and efficiency of such projects (Suzuki et al., 2022; Toledo et al., 2022).

The classification of natural frequency within the moderate range ($4<f_0<10$) suggests a moderate level of soil hardness in the research area. Soil stiffness, determined by natural frequency, plays a pivotal role in how seismic waves propagate through the ground. The moderate soil hardness, observed in tandem with seismic vulnerability assessments, indicates the need for tailored engineering solutions. Understanding the geological composition, specifically the identified Qv2 lithology, aids in predicting ground behavior during seismic events and guides construction practices for geothermal facilities (Gajek & Malinowski, 2021; Nibe & Matsushima, 2021).

The classification of peak ground acceleration as moderate (0.25<PGA<0.7) provides a quantitative measure of the ground shaking intensity. The correlation between PGA, magnitude values, and the proximity to injection wells and production wells indicates localized seismic risks. Higher PGA values signify greater risk potential, emphasizing the importance of establishing safety zones around critical geothermal infrastructure. This knowledge is essential for implementing appropriate safety protocols, designing structurally sound facilities, and safeguarding both workers and surrounding communities.

The identification of the seismic vulnerability index within the low classification (VI<10) signifies a relatively low susceptibility to surface soil layer deformation during earthquakes. This suggests that while the area experiences seismic activity, the ground deformation risk to surface structures is relatively low. However, it's crucial to note that this low vulnerability should not lead to complacency. Continuous monitoring and regular updates to vulnerability assessments are necessary to adapt to any changes in seismic patterns or geological conditions (Alkan & Akkaya, 2023; Sevilla et al., 2020).

The seismic susceptibility index, influenced significantly by maximum amplitude and natural frequency, underlines the need for a multidimensional approach to seismic risk assessment. Maximum amplitude reflects the energy released during seismic events, while natural frequency indicates the soil's inherent stiffness. Integrating these factors into vulnerability assessments provides a holistic view of the seismic landscape, enabling more accurate risk mitigation strategies and ensuring the resilience of geothermal operations (Ferrario et al., 2022; Menna et al., 2022).

The interplay between local magnitude, peak ground acceleration, and vulnerability index in the geothermal area underscores the complexity of seismic behavior. This research not only enhances our understanding of the region's seismicity but also provides a foundation for informed decision-making. By leveraging this knowledge, geothermal engineers and stakeholders can implement adaptive and effective strategies, ensuring the sustainable and safe exploitation of geothermal resources in seismic-prone regions. Continuous research, monitoring, and collaboration between geologists, seismologists, and engineers remain essential in navigating the intricate challenges posed by seismic activities in geothermal areas (Keil et al., 2022; Majidi Nezhad et al., 2021; Toledo et al., 2022).

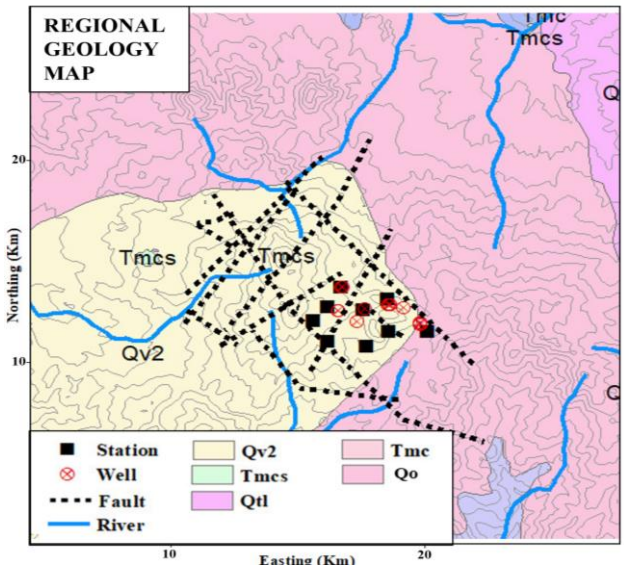

Figure 8. Research Area Geology Map

Conclusion

Intensive activities of geothermal injection and production can trigger microearthquakes. The microearthquake signal comes from dynamic fractures and fractures in the reservoir. The microearthquakes zone is located around the injection wells and production wells. The local magnitude impact on ground acceleration and seismic susceptibility index in this study has a moderate risk and can be categorized as safe. the integration of local magnitude, peak ground acceleration, and the seismic vulnerability index provides a comprehensive understanding of the seismic landscape in the geothermal area. This knowledge not only enhances our understanding of the region's geophysical behavior but also serves as a foundation for informed decision-making in geothermal energy operations and infrastructure development.

Acknowledgments

Various people have had helped the author in the process of making this paper so that the author can complete this research. The author would like to thank Institut Teknologi Sepuluh Nopember for providing data and making it easier for the author to conduct research.

Author Contribution

Author contributions include Widya Utama and Sherly A. Garini: focusing on methodology, reviewing, etc.; Rista F. Indriani: collecting data, processing data, analyzing data, and writing the original manuscript.

Funding

This research was privately funded by the authors.

Conflicts of Interest

The authors declare no conflict of interest.

References

Alkan, A., & Akkaya, İ. (2023). Investigation of site properties of the Çaldıran (Van, Eastern Turkey) settlement area using surface wave and microtremor methods. In *Journal of African Earth Sciences*, *197*. https://doi.org/10.1016/j.jafrearsci.2022.104737

Andinisari, R., Konstantinou, K. I., & Ranjan, P. (2021). Moment tensor inversion of microearthquakes along the Santorini-Amorgos zone: Tensile faulting and emerging volcanism in an extensional setting. *Journal of Volcanology and Geothermal Research*, *420*, 107394. https://doi.org/10.1016/j.jvolgeores.2021.107394

Bulo, D., Djayus, Supriyanto, & Hendrawanto, B. (2020). Penentuan Titik Epicenter dan Hypocenter Serta Parameter Magnitude Gempa Bumi Berdasarkan Data Seismogram. *Jurnal Geosains Kutai Basin*, *3*(1), 1–8. Retrieved from http://jurnal.fmipa.unmul.ac.id/index.php/geofis/article/view/597

Cao, R., Shi, J., Jia, Z., Cao, C., Cheng, L., & Liu, G. (2023). A modified 3D-EDFM method considering fracture width variation due to thermal stress and its application in enhanced geothermal system. *Journal of Hydrology*, *623*(May), 129749. https://doi.org/10.1016/j.jhydrol.2023.129749

Dwiyanti, N. E., Irnanda, V., N, E. S., Palupi, I. R., & Raharjo, W. (2020). Analisi Hubungan Magnitudo Gempa Bumi Terhadap Hasil Frekuensi Dominan Pada Rangkaian Gempa Aceh Upaya Mitigasi Bencana. *Jurnal Meteorologi Klimatologi dan Geofisika. 7*(3), 44–50. Retrieved from https://jurnal.stmkg.ac.id/index.php/jmkg/article/view/203

Elbshbeshi, A., Gomaa, A., Mohamed, A., Othman, A., & Ghazala, H. (2022). Seismic hazard evaluation by employing microtremor measurements for Abu Simbel area, Aswan, Egypt. In *Journal of African Earth Sciences*, *196*, 104734. https://doi.org/10.1016/j.jafrearsci.2022.104734

Esquivel-Mendiola, L. I., Calò, M., Tramelli, A., & Figueroa-Soto, A. (2022). Optimization of local scale seismic networks applied to geothermal fields. The case of the Acoculco caldera, Mexico. *Journal of South American Earth Sciences*, *119*. https://doi.org/10.1016/j.jsames.2022.103995

Ferrario, E., Poulos, A., Castro, S., de la Llera, J. C., & Lorca, A. (2022). Predictive capacity of topological measures in evaluating seismic risk and resilience of electric power networks. *Reliability Engineering and System Safety*, *217*, 108040. https://doi.org/10.1016/j.ress.2021.108040

Foytong, P., & Ornthammarath, T. (2020). Empirical seismic fragility functions based on field survey data after the 5 May 2014 Mae Lao (Northern Thailand) earthquake. *International Journal of Disaster Risk Reduction*, *42*, 101344. https://doi.org/10.1016/j.ijdrr.2019.101344

Gajek, W., & Malinowski, M. (2021). Errors in microseismic events locations introduced by neglecting anisotropy during velocity model calibration in downhole monitoring. *Journal of Applied Geophysics*, *184*. https://doi.org/10.1016/j.jappgeo.2020.104222

Gori, F., Paternoster, M., Barbieri, M., Buttitta, D., Caracausi, A., Parente, F., Sulli, A., & Petitta, M. (2023). Hydrogeochemical multi-component approach to assess fluids upwelling and mixing in shallow carbonate-evaporitic aquifers (Contursi area, southern Apennines, Italy). *Journal of Hydrology*, *618*, 129258. https://doi.org/10.1016/j.jhydrol.2023.129258

Guglielmi, Y., McClure, M., Burghardt, J., Morris, J. P., Doe, T., Fu, P., Knox, H., Vermeul, V., Kneafsey, T., Ajo-Franklin, J., Baumgartner, T., Beckers, K., Blankenship, D., Bonneville, A., Boyd, L., Brown, S., Burghardt, J. A., Chai, C., Chakravarty, A., … Zoback, M. D. (2023). Using in-situ strain measurements to evaluate the accuracy of stress estimation procedures from fracture injection/shut-in tests. *International Journal of Rock Mechanics and Mining Sciences*, *170*. https://doi.org/10.1016/j.ijrmms.2023.105521

Hendra, H., Efendi, R., & Rusydi H., M. (2019). Estimasi Karakteristik Dinamis Bawah Permukaan Menggunakan Refraksi Mikrotremor di Kota Palu. *Gravitasi*, *18*(1), 57–66. https://doi.org/10.22487/gravitasi.v18i1.13310

Hofmann, H., Zimmermann, G., Huenges, E., Regenspurg, S., Aldaz, S., Milkereit, C., Heimann, S., Dahm, T., Zang, A., Grigoli, F., Karvounis, D., Broccardo, M., Wiemer, S., Hjörleifsdóttir, V., Kristjánsson, B. R., Hersir, G. P., Ásgeirsdóttir, R. S., Magnússon, R., & Árnadóttir, S. (2021). Soft stimulation treatment of geothermal well RV-43 to meet the growing heat demand of Reykjavik. *Geothermics*, *96*, 102146. https://doi.org/10.1016/j.geothermics.2021.102146

Hopp, C., Sewell, S., Mroczek, S., Savage, M., & Townend, J. (2019). Seismic Response to Injection Well Stimulation in a High-Temperature, High-Permeability Reservoir. *Geochemistry, Geophysics, Geosystems*, *20*(6), 2848–2871. https://doi.org/10.1029/2019GC008243

Hopp, C., Sewell, S., Mroczek, S., Savage, M., & Townend, J. (2020). Seismic response to evolving injection at the Rotokawa geothermal field, New

Zealand. *Geothermics*, *85*, 101750. https://doi.org/10.1016/j.geothermics.2019.101750

Jun, S. C., Jung, D. I., Lee, C. H., & Cho, B. H. (2023). Experimental and numerical investigation of seismic response of access floors based on shake-table tests using 2-story steel moment frame. *Journal of Building Engineering*, *77*(July), 107474. https://doi.org/10.1016/j.jobe.2023.107474

Keil, S., Wassermann, J., & Megies, T. (2022). Estimation of ground motion due to induced seismicity at a geothermal power plant near Munich, Germany, using numerical simulations. *Geothermics*, *106*, 102577. https://doi.org/10.1016/j.geothermics.2022.102577

Kim, K. Il, Min, K. B., Kim, K. Y., Choi, J. W., Yoon, K. S., Yoon, W. S., Yoon, B., Lee, T. J., & Song, Y. (2018). Protocol for induced microseismicity in the first enhanced geothermal systems project in Pohang, Korea. *Renewable and Sustainable Energy Reviews*, *91*, 1182–1191. https://doi.org/10.1016/j.rser.2018.04.062

Kinscher, J. L., Broothaers, M., Schmittbuhl, J., de Santis, F., Laenen, B., & Klein, E. (2023). First insights to the seismic response of the fractured Carboniferous limestone reservoir at the Balmatt geothermal doublet (Belgium). *Geothermics*, *107*, 102585. https://doi.org/10.1016/j.geothermics.2022.102585

Kowsari, M., Halldorsson, B., Snæbjörnsson, J., & Jónsson, S. (2021). Effects of different empirical ground motion models on seismic hazard maps for North Iceland. *Soil Dynamics and Earthquake Engineering*, *148*, 106513. https://doi.org/10.1016/j.soildyn.2020.106513

Li, B., Xu, N., Xiao, P., Xia, Y., Zhou, X., Gu, G., & Yang, X. (2023). Microseismic monitoring and forecasting of dynamic disasters in underground hydropower projects in southwest China: A review. *Journal of Rock Mechanics and Geotechnical Engineering*, *15*(8), 2158–2177. https://doi.org/10.1016/j.jrmge.2022.10.017

Liu, X., Jin, Y., & Lin, B. (2022). Classification and evaluation for stimulated reservoir volume (SRV) estimation models using microseismic events based on three typical grid structures. *Journal of Petroleum Science and Engineering*, *211*, 110169. https://doi.org/10.1016/j.petrol.2022.110169

Lobos Lillo, D., Delgado, F., Pritchard, M. E., Cardona, C., Franco, L., Pedreros, G., & Amigo, A. (2023). Documenting surface deformation at the first geothermal power plant in South America (Cerro Pabellón, Chile) by satellite InSAR time-series. *Journal of Volcanology and Geothermal Research*, *441*, 107869. https://doi.org/10.1016/j.jvolgeores.2023.107869

Mahjour, S. K., & Faroughi, S. A. (2023). Risks and uncertainties in carbon capture , transport , and storage projects : A comprehensive review. *Gas Science and Engineering*, *119*, 205117. https://doi.org/10.1016/j.jgsce.2023.205117

Maimun, A. K., Silvia, U. N., & Ariyanto, P. (2020). Analisis Indeks Kerentanan Seismik, Periode Dominan, Dan Faktor Amplifikasi Menggunakan Metode Hvsr Di Stageof Tangerang. *Jurnal Meteorologi Klimatologi dan Geofisika,* 7(2), 24-30. Retrieved from https://jurnal.stmkg.ac.id/index.php/jmkg/article/view/194

Majidi Nezhad, M., Nastasi, B., Groppi, D., Lamagna, M., Piras, G., & Astiaso Garcia, D. (2021). Green Energy Sources Assessment Using Sentinel-1 Satellite Remote Sensing. *Frontiers in Energy Research*, *9*, 1–20. https://doi.org/10.3389/fenrg.2021.649305

Menna, C., Felicioni, L., Negro, P., Lupíšek, A., Romano, E., Prota, A., & Hájek, P. (2022). Review of methods for the combined assessment of seismic resilience and energy efficiency towards sustainable retrofitting of existing European buildings. *Sustainable Cities and Society*, *77*. https://doi.org/10.1016/j.scs.2021.103556

Midzi, V., Pule, T., Manzunzu, B., Mulabisana, T., Zulu, B. S., & Myendeki, S. (2020). Improved earthquake location in the gold mining regions of south africa using new velocity models. *South African Journal of Geology*, *123*(1), 35–58. https://doi.org/10.25131/sajg.123.0008

Mihaylov, A., El Naggar, H., Mihaylov, D., & Dineva, S. (2019). Approximate analytical HVSR curve using multiple band-pass filters and potential applications. *Soil Dynamics and Earthquake Engineering*, *127*, 105840. https://doi.org/10.1016/j.soildyn.2019.105840

Nibe, T., & Matsushima, J. (2021). Monitoring of seismic attenuation change associated with vapor-liquid phase transition using time-lapse reflection seismic data in Kakkonda geothermal field, Japan. *Geothermics*, *91*, 102034. https://doi.org/10.1016/j.geothermics.2020.102034

Núñez, D., Núñez-Cornú, F. J., & Rowe, C. A. (2022). Recent seismicity at Ceboruco Volcano (Mexico). *Journal of Volcanology and Geothermal Research*, *421*. https://doi.org/10.1016/j.jvolgeores.2021.107451

Okamoto, K., Imanishi, K., & Asanuma, H. (2022). Structures and fluid flows inferred from the microseismic events around a low-resistivity anomaly in the Kakkonda geothermal field,

Northeast Japan. *Geothermics*, *100*, 102320. https://doi.org/10.1016/j.geothermics.2021.102320

Ramirez, R. A., Lee, G. J., Choi, S. K., Kwon, T. H., Kim, Y. C., Ryu, H. H., Kim, S., Bae, B., & Hyun, C. (2022). Monitoring of construction-induced urban ground deformations using Sentinel-1 PS-InSAR: The case study of tunneling in Dangjin, Korea. *International Journal of Applied Earth Observation and Geoinformation*, *108*, 102721. https://doi.org/10.1016/j.jag.2022.102721

Ryu, H. S., Kim, H., Lee, J. Y., Kaown, D., & Lee, K. K. (2022). Abnormal groundwater levels and microbial communities in the Pohang Enhanced Geothermal System site wells pre- and post-Mw 5.5 earthquake in Korea. *Science of the Total Environment*, *810*, 152305. https://doi.org/10.1016/j.scitotenv.2021.152305

Sevilla, W. I., Jumawan, L. A., Clarito, C. J., Quintia, M. A., Dominguiano, A. A., & Solidum, R. U. (2020). Improved 1D velocity model and deep long-period earthquakes in Kanlaon Volcano, Philippines: Implications for its magmatic system. *Journal of Volcanology and Geothermal Research*, *393*, 106793. https://doi.org/10.1016/j.jvolgeores.2020.106793

Shim, H. J., Kim, J., Cheon, M. S., & Pak, S. (2023). A comparison study on the derivation of in-structure FRS during seismic events for application of ITER upper port 18. *Fusion Engineering and Design*, *191*, 113771. https://doi.org/10.1016/j.fusengdes.2023.113771

Sungkowo, A. (2018). Perhitungan Nilai Percepatan Tanah Maksimum Berdasar Rekaman Sinyal Accelerograph di Stasiun Pengukuran UNSO Surakarta. *Indonesian Journal of Applied Physics*, *8*(1), 43. https://doi.org/10.13057/ijap.v8i1.14326

Suzuki, Y., Akatsuka, T., Yamaya, Y., Watanabe, N., Okamoto, K., Osato, K., Kajiwara, T., Ogawa, Y., Mogi, T., Tsuchiya, N., & Asanuma, H. (2022). Estimation of an ultra-high-temperature geothermal reservoir model in the Kakkonda geothermal field, northeastern Japan. *Geothermics*, *105*, 102525. https://doi.org/10.1016/j.geothermics.2022.102525

Tang, S., Li, J., Tang, L., & Zhang, L. (2023). Microseismic monitoring and experimental study on rockburst in water-rich area of tunnel. *Tunnelling and Underground Space Technology*, *141*, 105366. https://doi.org/10.1016/j.tust.2023.105366

Tao, J., Shi, A. C., Li, H. T., Zhou, J. W., Yang, X. G., & Lu, G. Da. (2021). Thermal-mechanical modelling of rock response and damage evolution during excavation in prestressed geothermal deposits. *International Journal of Rock Mechanics and Mining Sciences*, *147*, 104913. https://doi.org/10.1016/j.ijrmms.2021.104913

Toledo, T., Obermann, A., Verdel, A., Martins, J. E., Jousset, P., Mortensen, A. K., Erbas, K., & Krawczyk, C. M. (2022). Ambient seismic noise monitoring and imaging at the Theistareykir geothermal field (Iceland). *Journal of Volcanology and Geothermal Research*, *429*, 107590. https://doi.org/10.1016/j.jvolgeores.2022.107590

Utama, W., Warnana, D. D., & Garini, S. A. (2020). Identification of Micro-Earthquake Hypocentre using Geiger and Coupled Velocity-Hypocentre Methods. *International Journal on Advanced Science, Engineering and Information Technology*, *11*(1), 350–355. https://doi.org/10.18517/ijaseit.11.1.10589

Wamriew, D., Charara, M., & Pissarenko, D. (2022). Joint event location and velocity model update in real-time for downhole microseismic monitoring: A deep learning approach. *Computers and Geosciences*, *158*, 104965. https://doi.org/10.1016/j.cageo.2021.104965

Xie, J., Wang, J., & Liu, X. (2021). The role of fracture networks randomness in thermal utilization of enhanced geothermal system. *International Communications in Heat and Mass Transfer*, *126*, 105414. https://doi.org/10.1016/j.icheatmasstransfer.2021.105414

Yoo, H., Park, S., Xie, L., Kim, K. Il, Min, K. B., Rutqvist, J., & Rinaldi, A. P. (2021). Hydro-mechanical modeling of the first and second hydraulic stimulations in a fractured geothermal reservoir in Pohang, South Korea. *Geothermics*, *89*, 101982. https://doi.org/10.1016/j.geothermics.2020.101982

Yue, G., Li, X., & Zhang, W. (2023). Risk assessment of earthquakes induced during HDR development: A case study in the Gonghe Basin, Qinghai Province, China. *Geothermics*, *111*, 102721. https://doi.org/10.1016/j.geothermics.2023.102721

Zhang, C., Peng, Z., Liu, X., & Li, C. (2023). Spatio-temporal variations of shallow seismic velocity changes in Salton Sea Geothermal Field, California in response to large regional earthquakes and long-term geothermal activities. *Earthquake Research Advances*, *3*(2), 100178. https://doi.org/10.1016/j.eqrea.2022.100178

Zhou, Y., Yue, H., Zhou, S., Fang, L., Zhou, Y., Xu, L., Liu, Z., Wang, T., Zhao, L., & Ghosh, A. (2022). Microseismicity along Xiaojiang Fault Zone (Southeastern Tibetan Plateau) and the characterization of interseismic fault behavior. *Tectonophysics*, *833*, 229364. https://doi.org/10.1016/j.tecto.2022.229364